A superconductor-insulator-normal metal bolometer with microwave readout suitable for large-format arrays

D. R. Schmidt[a], A. M. Clark[b], W. D. Duncan[b], K. D. Irwin[b], N. Miller[b], J. N. Ullom[b], and K. W. Lehnert[a]
[a] *JILA, National Institute of Standards and Technology and Department of Physics, University of Colorado, Boulder, Colorado 80309*
[b] *National Institute of Standards and Technology, Boulder, Colorado 80305*
(Dated: November 1, 2004)

We demonstrate high bandwidth and low-noise readout of a superconductor-insulator-normal metal-insulator-superconductor hot-electron bolometer element. We measure a noise equivalent temperature of better than 0.6 μK/Hz$^{1/2}$ and infer an electrical noise equivalent power of 7 $\times$ 10^{-17} W/Hz$^{1/2}$ for a normal-metal volume of 4.5 μm^3 at an operating temperature of 270 mK. Using a pulsed bias technique we measure a thermal time constant of 1.2 μs at 270 mK. The microwave readout method we employ is compatible with large-format arrays of 10^3-10^5 pixels required by future far-infrared space and ground-based observatories.

The desire for sensitive bolometers has forced the fabrication of detectors with ever weaker links to thermal reservoirs. To this end, operating temperatures have been lowered well below 1 K, and microfabrication techniques have been employed to mechanically suspend detectors.[1,2] At the lowest temperatures, electrons in a metal naturally decouple from their local phonon environment[3–6] with a resulting weak electron-phonon thermal conductance that provides far greater thermal isolation than can be achieved with a nano-suspension.[7–9] Detectors that exploit this decoupling can meet the pressing need for ultra-low noise equivalent power (NEP) bolometers and energy-resolving photon-counting calorimeters.

Major astronomical applications of bolometers require large-format (10^3-10^5 pixels) arrays of detectors with NEPs lower than 5 $\times$ 10^{-18} W/Hz$^{1/2}$ for deep-space mapping in the far-infrared (1 mm - 10 μm) wavelength band. Furthermore, it is desirable for some applications to be able to count photons in this waveband. Since detector thermal time constants can be $\approx$ 1 μs, instantaneous measurement bandwidths of 10 MHz are required. These criteria set stringent requirements on both the individual detector elements and the methods used to read-out the array. In the Letter, we demonstrate a microwave based electron thermometry that could read out large scale arrays of ultra-low NEP bolometers.

Simple analysis reveals the potential of bolometers based on electron-phonon decoupling. Direct detector performance is limited ultimately by thermal fluctuations across the relevant thermal conductivity, G. The thermal-fluctuation noise limit for the noise equivalent power of a bolometric detector at a temperature, T, is given by

$$\mathrm{NEP_{ph}} = \sqrt{4\mathrm{k_B T^2 G}}. \quad (1)$$

The thermal conductivity is dominated by the electron-phonon contribution, G_{e-p},

$$G_{e-p} = (n+1)\Sigma V T^n, \quad (2)$$

where Σ is a material dependent parameter, V is the metal volume, and the power-law exponent n is typically $\approx$ 4 for common metals such as Cu, Au, and normal-state Al.[3,4,6] The thermal fluctuation noise limit for a hot electron bolometer is then

$$\mathrm{NEP_{ph}} = \sqrt{20\mathrm{k_B}\Sigma\mathrm{V}}\,\mathrm{T}^3. \quad (3)$$

Since the parameter Σ is 1-2 nW/(μm^{3}K^5), application-critical NEPs of 10^{-18}-10^{-20} W/Hz$^{1/2}$ are achievable with metal volumes of 0.1-1.0 μm^3 and operating temperatures of 50-300 mK.[5,6] The major technological challenge is monitoring the electron temperature; the thermometry must achieve low noise and maintain thermal isolation. For this task we

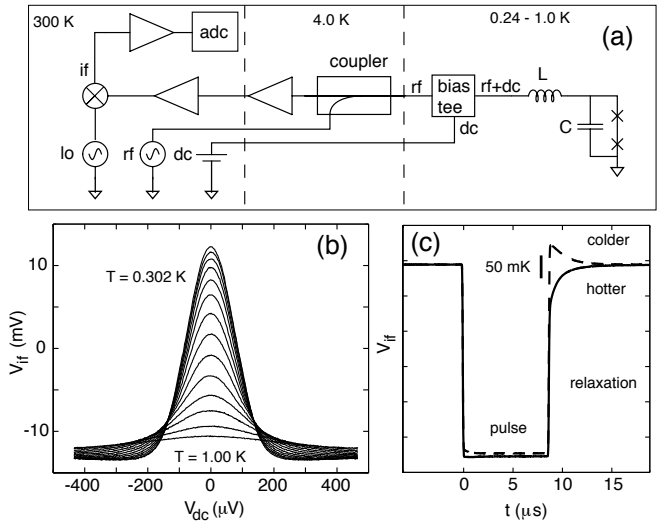

FIG. 1: (a) Circuit schematic. The microwave carrier signal (rf) is delivered to the device through a directional coupler. An inductor and the intrinsic device capacitance are used to impedance-match to the microwave amplifier chain. The intermediate-frequency output of the mixer (if) is further amplified and digitized (adc). A bias tee permits dc biasing. (b) Detector response: the intermediate-frequency voltage response of the reflectometer as a function of dc bias for a range of temperatures, 240-700 mK. (c) Pulse response. A square pulse (7 μs width) is applied to the dc bias line at time $t = 0$. The response to two different pulse heights is shown. After one pulse (solid line) the electronic temperature is hotter than it was initially. The other pulse (dashed line) results in a colder temperature.

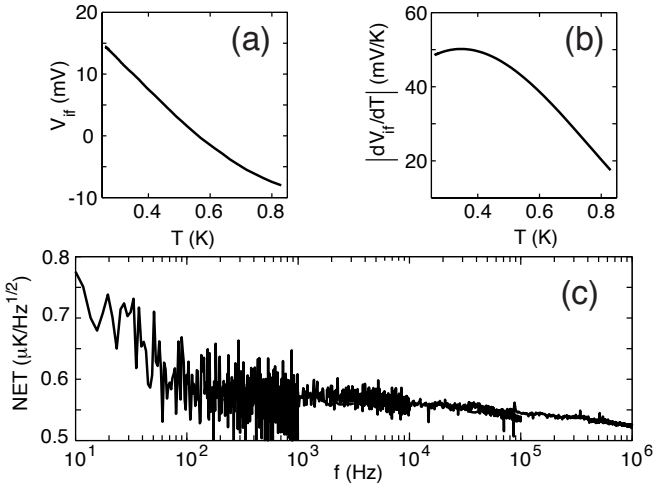

FIG. 2: (a) Detector V_{if} response for zero dc bias and $\approx$ 30 pW incident carrier power. (b) Measured responsivity dV_{if}/dT as a function of temperature. (c) Measured NET at 270 mK. The NET of the device is less than 0.6 μK/Hz$^{1/2}$ over the 100 Hz-1 MHz band (note that zero is suppressed). The NET is given by the product of the measured voltage noise V_N and the inverse responsivity, NET = $V_N(dV_{if}/dT)^{-1}$.

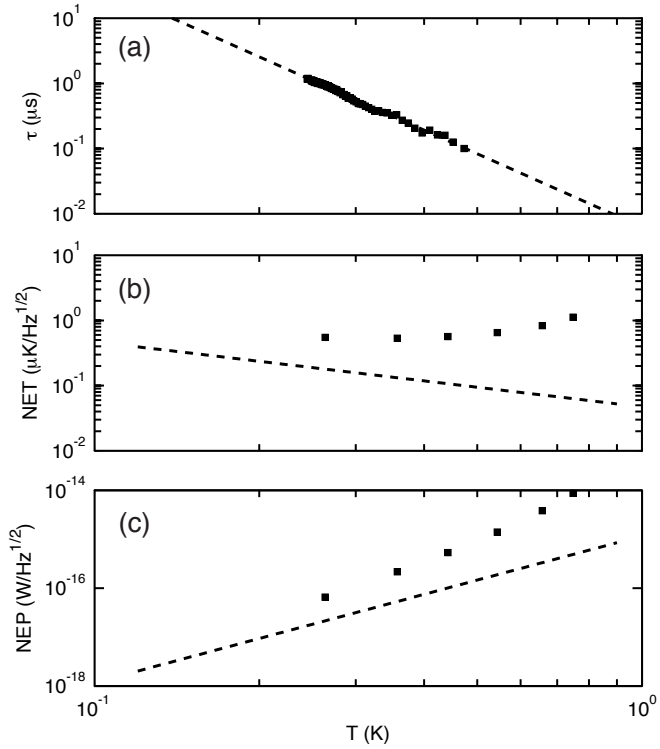

FIG. 3: Summary of device performance. (a) Measured thermal time constant with a power-law fit (dashed line). (b) Measured NET and estimated thermal-fluctuation-limited NET (dashed line). (c) Inferred NEP and estimated thermal-fluctuation-limited NEP (dashed line).

employ superconducting tunnel junction technology, specifically the radio-frequency superconductor-insulator-normal metal (rf-SIN) thermometer.

Superconductor-insulator-normal metal (SIN) junctions have already been proposed as sensitive thermometers for hot-electron bolometers.[10] The SINIS structure has two SIN junctions for thermometry and a thermally isolated normal-metal volume. While microwave readout of SIN thermometers has been demonstrated,[11,12] the initial measurements used a room-temperature microwave amplifier and achieved noise equivalent temperature (NET) of only 280 μK/Hz$^{1/2}$. However, it was projected that this rf-SIN thermometer could achieve temperature sensitivities below 1 μK/Hz$^{1/2}$. Here we obtain low-noise rf-SIN readout of a bolometer element with better than a five-hundred-fold improvement in NET than that previously reported.[11] While the bulk of the improvement is due to use of a cryogenic amplifier, we also achieve nearly a factor of four improvement from a lower device impedance. Our bolometers are fabricated with a wafer-scale process that can readily produce large-format arrays that can be integrated with the rf-SIN readout. The rf-SIN thermometer itself is inherently array compatible because of the ability to utilize frequency division multiplexing (FDM). We believe the implementation of the rf-SIN thermometer presented here can meet the design criteria of future focal-plane bolometer arrays.

The bolometer element we measured was a double-junction SINIS structure on an oxidized silicon substrate. Both the normal-metal and the superconducting leads are Al, with non-superconducting Al realized by adding a small (0.3%) Mn content to the normal-metal island. Our superconducting Al has an energy gap, $\Delta \approx 190$ μeV. The normal metal dimensions are 15 $\times$ 6.5 $\times$ 0.05 μm^3. The AlMn was oxidized and superconducting electrodes were added to form two tunnel junctions each with dimensions 5 $\times$ 5 μm^2. The combined normal-state resistance of the junctions is 70 Ω. The relatively thick (0.4 μm) Al counterelectrodes enable efficient electronic refrigeration.[13] These superconducting counterelectrodes can be readily integrated into THz scale antennas with high coupling efficiencies and wide bandwidths. In a typical process run, four thousand junctions are fabricated on a 75 mm Si wafer with near unity yield. From the normal metal volume (4.5 μm^3) and previously determined value of Σ = 1.1 nW/(μm^{3}K^5) for these materials,[13] we predict the thermal NET and NEP to be 0.2 μK/Hz$^{1/2}$ and 1.6$\times 10^{-17}$ W/Hz$^{1/2}$, respectively, at 270 mK.

At voltages where the device is temperature sensitive, below $2\Delta/e$, its dynamic resistance exceeds 1 kΩ. To improve the impedance match, we used an L-section matching circuit to transform the device impedance towards that of our 50 Ω cryogenic amplifier. The reactive components of the matching circuit [Fig. 1a] are a surface-mount inductor (68 nH), and the sum of the device capacitance ($\approx$ 1.0 pF) and the stray capacitance ($\approx$ 0.3 pF) between the inductor and the tunnel junctions. The inductance was chosen to achieve an LC resonance within the bandwidth of our amplifier (400-600 MHz).

In the rf-SIN technique, the SINIS device is measured by monitoring the microwave power reflected off of the matching circuit.[11,12,14] In this particular implementation, our device was mounted on the lowest-temperature stage of a ^{3}He

cryostat (base temperature $\approx$ 240 mK), and microwave power was delivered to the device through the coupled port of a directional coupler (30 dB coupling). The reflected signal was measured with a microwave amplifier. Both the amplifier and coupler were located in the liquid ^{4}He bath. The noise temperature of this amplifier is in the range 1.0 K to 4.5 K in the specified band. Low-frequency bias signals were applied to the device via a bias tee at the lowest-temperature stage. The output of the cryogenic amplifier was further amplified at room temperature, bandpass filtered, and detected using homodyne mixing. The resultant baseband voltage from intermediate-frequency port of the mixer (V_{if}) was amplified and digitized.

We measured the matching circuit resonance to be $\approx$ 450 MHz and found that its low Q ($\approx$ 3) provided modulation over the entire amplifier band. For the data presented here, the reflectometer was operated at 540 MHz where the amplifier noise was the lowest. The reflected signal response of the device (in terms of V_{if}) was measured as a function of device bias for a range of physical temperatures and the result is shown in Fig. 1(b). The nominal microwave power was 30 pW (-75 dBm). The local oscillator's phase and the carrier power were chosen to maximize temperature responsivity, dV_{if}/dT. We estimated the voltage swing due to the carrier signal to be $\approx$ 300 μV = 1.6 Δ/e. From Fig. 1(b) it is apparent the response is symmetric with respect to dc bias, and the largest change in response with respect to temperature occurs at zero dc bias. Therefore for operation as a thermometer the device should be held at zero dc bias with the additional benefit that the quadratic bias response provides a measure of immunity from bias noise sources.

Since our measurement bandwidth is $>$ 50 MHz, it exceeds the thermal bandwidth of the device, and direct measurement of the thermal time constant is possible. To measure the device time constant we used a pulse applied to the dc bias line. A large voltage pulse ($V_{pulse} > 2\Delta/e$) will heat the electronic system. During the pulse, the rf-SIN's temperature sensitivity is poor. Once the pulse is turned off, the bias across the device returns to zero on a time scale ($\approx$ 20 ns) set by the bandwidth of our matching circuit. However, the hot-electron population created by the bias pulse relaxes to the base temperature with a time scale set by the thermal time constant, τ_{ep}.

Figure 1(c) shows the response of the device to two pulses of different voltage levels. For the operating conditions, larger V_{if} corresponds to colder temperatures. It is clear that τ_{ep} is of order 1 μs. A pulse with $V_{pulse} >> 2\ \Delta/e$ causes heating, while a pulse with $V_{pulse} \approx 1.8\ \Delta/e$ causes cooling. The presence of cooling is not surprising; as mentioned previously, efficient electronic refrigeration has been observed in these devices. In fact, our carrier signal is providing some electronic refrigeration. We estimate the carrier signal alone cools the electronic temperature by $\approx$ 50 mK, and the pulse bias provides an additional $\approx$ 50 mK of cooling. Provided the total voltage bias (microwave plus dc) is kept below the gap voltage, the bias power acts to cool the normal metal, and this cooling compensates for Joule heating due to the bias or any radiation load. This unique trait of SIN junctions is highly desirable for ultra-low-temperature bolometers.

The measured V_{if} response as a function of temperature at zero dc bias is shown in Fig. 2(a). The derivative dV_{if}/dT is shown in Fig. 2(b). The input power is chosen to maximize the device response. Responsivity is preserved over the temperature range measured, 240-700 mK. Bolometers based on the this type of technology can therefore have significant dynamic range. The peak in responsivity at 300 mK is due to the parameters of the matching circuit and can be tailored to a particular operating condition. The measured noise in our signal and the measured responsivity are used to determine the NET. At a temperature of 270 mK we determine the NET to be less than 0.6 μK/Hz$^{1/2}$ over the 100 Hz-1 MHz band [Fig. 2(c)]. The NET rises to 0.8 μK/Hz$^{1/2}$ between 100 Hz and 1 Hz. There are at least two components which may cause this low frequency noise: noise on the bias line and fluctuations of the amplifier's gain. Bias noise can be attenuated with a cryogenic dc shunt in the bias line. Low frequency gain fluctuations can be accounted for with a simultaneous measurement of the amplifier gain.

We calculate expected device performance by solving a set of coupled differential equations that describe the thermal and electrical properties of the device and measurement circuit. These lengthy calculations, which will be fully described elsewhere, predict that the detector output noise temperature is only 0.1 K. Hence, our noise measurements are amplifier limited and the measured NET corresponds to an amplifier noise temperature of $\approx$ 1.5 K. However, the output noise temperature of the device can be increased by reducing its volume and lowering the phonon temperature. The output noise temperature set by thermal fluctuations of a 1 μm^3 device operating at 240 (150) mK is predicted to be 0.9 (2.5) K. Hence, performance near the fundamental limit set by Eq. 3 is possible.

Figure 3 summarizes the experimentally determined bolometric performance. Bias-pulse data were used to determine the thermal time constant of the device as a function of physical temperature. The thermal relaxation due to each pulse was fitted to the solution of a differential equation that assumes power-law behavior for G_{e-p}.[12] The extracted thermal time constant shown in Fig. 3(a) follows a $T^{-3.7}$ power-law (dashed line) and ranges from 1.2 μs to below 0.1 μs over the measured temperature range. The data for the lowest temperatures are better fit by T^{-3}. As shown in Fig. 3b, the NET increases with temperature since responsivity decreases above 300 mK and the amplifier is the dominant source of noise. The measured NET as a function of temperature and the electron-phonon thermal conductance given by Eq. 2 are used to infer the electrical NEP [Fig. 3c][15].

Figure 3 can be used to estimate the energy resolution ($\Delta E = \mathrm{NEP}\tau_{e-p}^{1/2}$) of our detector for photon-counting applications. In this case, we gain a significant benefit due to the relatively short thermal time constant of $\approx$ 1 μs. For equivalent NEP, the faster detector will be able to count lower energy photons since the peak power generated by photon absorption will be higher. For our measured parameters, the device presented here should be able to detect a 60 THz photon with a signal-to-noise ratio of unity and a reduction of volume factor of ten will decrease the threshold to 6 THz.

Microwave readout techniques will enable focal planes with 10^3-10^5 sensing elements. Very large numbers of detec-

tors can be monitored with one microwave amplifier and one coaxial cable running to the focal plane if the resonant circuits are appropriately distributed in frequency and narrow enough in bandwidth. FDM is being investigated for arrays of single-electron transistors,[16] SQUIDS,[17] and kinetic-inductance detectors.[18] Resonant circuits built from components with intrinsic Q values of 1,000 (10,000) will enable 100 (1,000) SINIS detectors to be measured with a single amplifier. Hence, an instrument with 10-100 microwave amplifiers can read 10^3-10^5 sensors. A advantage of microwave FDM is that the physical size of the reactive components is compact,[19] so the resonant circuits can easily fit within the focal plane.

In summary, we have demonstrated measurements of a SINIS bolometer that show an electrical NEP within a factor of 4 of the thermal-fluctuation limit over a bandwidth that significantly exceeds the thermal bandwidth, $1/2\pi\tau_{e-p}$. Furthermore, our microwave reflectometer readout is compatible with device-limited noise measurements of large-format arrays (10^3-10^5 pixels) of ultra-low NEP bolometers. We believe these technologies offer a direct path to the focal planes required for next-generation far-infrared observatories. Additionally, we foresee delivering far-infrared photon counters in the near future.

We acknowledge assistance from A. Williams and support from NASA's Cross-Enterprise Technology Development Program. We also thank the staff of JILA's instrument and electronics shops for their technical support.

[1] S. H. Moseley, J. C. Mather, and D. McCammon, J. Appl. Phys **56**, 5 (1984).
[2] A. Szymkowiak, R. Kelley, G. Madejski, H. Moseley, R. Schoelkopf, B. Edwards, M. Juda, D. McCammon, M. Skinner, and J. Zhang, Rev. Sci. Inst. **60**, 7 (1989).
[3] W. A. Little, Can. J. Phys. **37**, 334 (1959).
[4] V. F. Gantmakher, Rep. Prog. Phys. **37**, 317 (1974).
[5] M. L. Roukes, M. R. Freeman, R. S. Germain, R. C. Richardson, and M. B. Ketchen, Phys. Rev. Lett. **55**, 422 (1985).
[6] F. C. Wellstood, C. Urbina, and J. Clarke, Phys. Rev. B **49**, 5942 (1994).
[7] K. Schwab, E. A. Henriksen, J. M. Worlock, and M. L. Roukes, Nature **404**, 974 (2000).
[8] C. S. Yung, D. R. Schmidt, and A. N. Cleland, Appl. Phys. Lett. **81**, 31 (2002).
[9] A. N. Cleland, D. R. Schmidt, and C. S. Yung, Phys. Rev. B **64**, 172301 (2001).
[10] M. Nahum and J. M. Martinis, Appl. Phys. Lett. **63**, 3075 (1993).
[11] D. R. Schmidt, C. S. Yung, and A. N. Cleland, Appl. Phys. Lett. **83**, 1002 (2003).
[12] D. R. Schmidt, C. S. Yung, and A. N. Cleland, Phys. Rev. B **69**, 140301 (2004).
[13] A. M. Clark, A. Williams, S. T. Ruggiero, M. L. van den Berg, and J. N. Ullom, Appl. Phys. Lett. **84**, 625 (2004).
[14] R. J. Schoelkopf, P. Wahlgren, A. A. Kozhevniv, P. Delsing, and D. E. Prober, Science **280**, 1238 (1998).
[15] While the functional form of G_{e-p} is certain, cooling by the microwave bias reduces T_e below T_p. Our inferred NEP is calculated using G_{e-p} at T_p. Since $T_e < T_p$, this choice will be a modest over estimate of the NEP.
[16] T. R. Stevenson, F. A. Pellerano, C. M. Stahle, K. Aidala, and R. J. Schoelkopf, Appl. Phys. Lett. **80**, 3012 (2002).
[17] K. D. Irwin and K. W. Lehnert, Appl. Phys. Lett. **85**, 2107 (2004).
[18] P. K. Day, H. G. LeDuc, B. A. Mazin, A. Vayonakis, and J. Zmuidzinas, Nature **425**, 817 (2003).
[19] J. N. Ullom, M. F. Cunningham, T. Miyazaki, S. E. Labov, J. Clarke, T. M. Lanting, A. T. Lee, P. L. Richards, J. Yoon, and H. Spieler, IEEE Trans. Appl. Supercon. **13**, 643 (2003).